The following publication X. Zhang et al., "Yen's Algorithm-Based Charging Facility Planning Considering Congestion in Coupled Transportation and Power Systems," in IEEE Transactions on Transportation Electrification, vol. 5, no. 4, pp. 1134-1144, Dec. 2019 is available at https://doi.org/10.1109/TTE.2019.2959716

Yen's Algorithm Based Charging Facility Planning Considering Congestion in Coupled Transportation and Power Systems

Xian Zhang, *Member*, *IEEE*, Peiling Li, Jiefeng Hu, *Senior Member*, *IEEE*, Ming Liu, Guibin Wang, *Member*, *IEEE*, Jing Qiu, *Member*, *IEEE*, K. W. Chan, *Senior Member*, *IEEE*

***Abstract*—To promote the penetration of electric vehicles (EVs), a charging facility (CF) planning model based on Yen's algorithm is proposed for coupled transportation and distribution systems considering traffic congestion. This model not only takes into account the influence of new CFs on the power system, but also considers the impact of CF locations on traffic flow distribution and congestion level in the transportation system. Yen's algorithm is innovatively employed to offer multiple possible choices for EV drivers' route-selection considering CF locations determined in traffic flow assignment model. Overall, the total cost of both distribution and transportation systems is minimized to obtain the optimal CF planning results. For the distribution system, generation cost, energy loss and penalty cost for voltage deviation are included. For the transportation system, the main objective is to ensure EVs can reach their destinations at the lowest cost, while the travel time due to different path selections and the delay time caused by congestion can be minimized. Finally, a comprehensive case study on the integrated IEEE 30-bus and a 25-node transportation system is conducted to validate our approach.**

***Index Terms*—Distribution System Planning, Charging Facility, EV flow, Yen's algorithm.**

NOMENCLATURE

Abbreviations:

CF	Charging facility
DS	Distribution system
EV	Electric Vehicle
FCS	Fast charging station
BSS	Battery swapping station
TS	Transportation System
O-D	origin-destination

Sets, Index and Parameters:

Ω^A, Ω^Z	Set of the coefficients of piecewise linear equation
Ω^{GP}	Set of the end/break-points of piecewise linear equation
Ω^{ND}	Set of nodes in DS
Ω^{LD}	Set of feeders in DS
Ω^T	Set of time intervals
Ω^τ	Set of departure time
Ω^{PT}	Set of O-D pairs
Ω^{LT}	Set of links on selected path for each O-D pair
Ω^H	Set of candidate CFs
t	Index of time intervals
τ	Index of departure time
h	Index of candidate CF
i,j	Index of DS node
ij	Index of DS feeders
r,s	Index of the origin and the destination
rs	Index of O-D pair
l	Index of TS link
f_τ^{rs}	EV flow from origin r to destination s departs at time τ
T_l^0	Free travel time on link l
T_{rs}^0	Free travel time from origin r to the destination s
cap_l	Capacity of link l
v_{max}	Max traveling speed on link l
R_{veh}	Cruising range of an EV
c^{tra}, c^{del}, c^{fail}	Coefficients of travel time cost, delay cost and travel failure cost
$a_{n,i}$, $z_{n,i}$	Coefficients of piecewise linear equation
P_{xn}	End/break-points of piecewise linear equation
$P_{i,t}^D$	Active power at DS node i at time t
G_{ij}, B_{ij}	Real and imaginary parts of the node admittance matrix
c^{VD}	Voltage deviation cost
c^{pl}	Power loss cost
$U_{i,rating}$	The voltage rating at DS nodes
U_i^{min}, U_i^{max}	Voltage upper and lower limits of DS node i
$S_{i,max}^{GEN}$	Apparent power capacity of the substation on node i
S_{ij}^{max}	Designed transfer capacity of feeder ij
p^{EV}	Charging power of EV
EC^{EV}	*EV power consumption per mile*
T_{qu}	Queueing time at FCS or BSS
L	The distance between node r to the first CF or the distance between two adjacent CFs
N^F, N^B	The number of FCSs and BSSs to be built
T	Total time intervals

This work is supported in part by Hong Kong Research Grants Council under Projects PolyU252040/17E and PolyU152064/19E, and in part by The Hong Kong Polytechnic University under Projects 1-ZE7J and G-YBZ4.

Xian Zhang, Jiefeng Hu, Ming Liu and K. W. Chan are with the Department of Electrical Engineering, The Hong Kong Polytechnic University, Hung Hom 999077, Hong Kong. (e-mail: eexianzhang@outlook.com; jerry.hu@polyu.edu.hk; leo.m.liu@connect.polyu.hk; eekwchan@polyu.edu.hk).

Peiling Li and Guibin Wang are with the College of Mechatronics and Control Engineering, Shenzhen University, Shenzhen 518060, China. (e-mail: lingzoro@163.com; wanggb@szu.edu.cn).

Jing Qiu is with the School of Electrical and Information Engineering, The University of Sydney, Sydney, NSW 2006, Australia. (e-mail: qiujing0322@gmail.com).

(Corresponding Author: Jiefeng Hu)

Variables:

F	The objective function
F_T	The EV transportation cost in TS
F_E	The operation cost in DS
f_{tra}	The overall travel time cost
f_{del}	The total delay cost
f_{fail}	The travel failure cost
f_{gen}	Generation cost
f_{vd}	The total penalty cost for voltage diviation
f_{pl}	Power loss cost
$C_{i,t}^{GEN}$	Generation cost on DS node i at time t
$U_{i,t}$,$U_{j,t}$	Voltage magnitudes of bus i and j at time t
$\theta_{ij,t}$	Phase angle deviation of branch ij at time t
$P_{i,t}^{GEN}$, $Q_{i,t}^{GEN}$	The active power and reactive power of the generator on node i in time t
$P_{i,t}^{D}$	Active power at DS node i at time t
$P_{ij,t}$, $Q_{ij,t}$	The active power and reactive power of branch ij at time t
$P_{i,t}^{CF}$	Active power of CF on node i at time t
$P_{i,t}^{BSS}$, $P_{i,t}^{FCS}$	Active power of BSS/FCS on node i at time t
$f_{i,t}^{rs}$	EV flow from origin r to destination s on node i at time t
$T_{rs,\tau}^{del}$	Total delay time of EV flow f_{τ}^{rs}
$T_{rs,\tau}^{tra}$	Total travel time of EV flow f_{τ}^{rs}
$T_{l}^{rs,\tau}$	Travel time of EV flow f_{τ}^{rs} on link l
$T_{h}^{rs,ch}$	Charging time of EV flow f_{τ}^{rs} at candidate CF h
$x_{l,t}$	the sum of EV flow on link l at time t
δ_{l}^{rs}	Binary decision variable for whether EV flow f_{τ}^{rs} could travel on link l
γ_{τ}^{rs}	Binary decision variable for whether the EV flow f_{τ}^{rs} could complete its trip
φ_{h}^{rs}	Binary decision variable for whether EV flow f_{τ}^{rs} has charged at the hth candidate CF.
u_i^F , u_i^B	Binary decision variable for whether a FCS or BSS will be constructed on node i

I. Introduction

A. Motivation

Electric vehicles (EVs) play an important role in reducing carbon emissions if more electricity can be supplied by renewable energy. In addition, EV batteries can be controlled to achieve smart charging and have the potential to respond to energy market signals [1]. In practice, many factors hinder the deployment of EVs [2], such as EV price, the development of EV batteries and charging infrastructure planning. The relationship between these factors and 30 national EV market shares are examined using multiple linear regression analysis in [3]. Their results show that charging infrastructure planning is strongly related to EV market share, which is the key issue addressed in this work.

B. Literature Review

Charging facility (CF) planning has been separately studied by the power system community and the transportation community over the past decades [4]. However, the adequacy and convenience of charging service provided by CFs in the transportation system (TS) should be accessed, and the influence of CFs on the power system should not be neglected. In recent years, researchers have investigated CF planning in the coupled traffic-power system [5] -[14]. These CF planning models can be divided into two categories: single-objective planning and multi-objective planning. Models proposed in [5], [8] and [12] are multi-objective, whereas the models mentioned in [6], [7], [9], [10], [11], [13] and [14] belong to single-objective type. In [5], a multiobjective CF planning method which maximizes charging service ability while minimizing power losses and voltage deviations in distribution systems (DSs) is proposed. In [6], EV CFs are planned utilizing advanced evaluation method with the consideration of uncertainties. In [7], to determine the site and the size of the charging stations, net present value and life cycle cost are considered in the planning model. The multi-objective model developed in [8] minimizes the overall annual cost of investment and energy losses simultaneously with the maximization of the annual traffic flow captured by CFs. In [9], the economic charging station planning model is built simultaneously taking into account traffic constraints and load profile templates. In [10], the proposed comprehensive planning model determines the optimal expansion strategies for both transportation network and power distribution network, including sites and sizes of new charging stations, charging spots, transportation network lanes, and power distribution network lines. In [11], fast charging station siting and sizing in coupled transportation and power networks is investigated to increase social welfare. In [12], the developed CF planning model aims to reduce the power losses and voltage deviation of the distribution system, and then increase the EV flow served by CFs considering permissible waiting time and service radius of CF. In [13], the CF location model is investigated to minimize the average driving cost and the minimum line costs between CF and the distribution nodes. [14] developed a CF location planning model taking into account the impacts on the critical power grid assets.

In [5], EV Expected Energy Not Supplied (EVEENS) which is defined as the annual traffic flow not charged by the CFs is proposed for the first time to quantify the service ability of CFs in the EV charging stations planning procedure in the coupled traffic-power system. Motivated by [5], many proposed CF planning models considers the service ability of CFs in CF planning procedures [6]-[14]. The service capacity of CFs is highly related to the traffic flow passing by, while traffic flow assignment depends on drivers' route-selection. The traffic assignment model assuming that drivers only choose the shortest path between the origin and destination is a commonly used traffic flow assignment model, which has been utilized in [5]-[6], [11]-[12], [14] and many other unmentioned references. Actually, this model is more suitable for the transportation network without any congestion [15]. The reality is that when the battery capacity is not sufficient to cover the shortest route, drivers are willing to take detours to charge their EVs and then continue to drive to the destination. There are some other proposed traffic flow assignment models [7]-[10] [13] [16]. In [7], [13] and [16], the CF planning model uses the historical traffic flow data to integrate distribution network constraint, user constraints and traffic flow captured constraints. However, obtaining such data may be costly for some target planning

networks, and the historical data may not be readily available for other practical applications. In [8], the user equilibrium based traffic assignment model is introduced in this strategy to obtain traffic flow data. In [9], the system optimization model is utilized to generate and assign the traffic flow in economic CF planning. In [10], an unconstrained traffic assignment model is developed to explicitly capture the steady-state distribution of traffic flows. However, all the traffic assignment model (route-choice models) mentioned in references [5]-[14] generate traffic assignment data independently before CFs planning procedures without considering the impact of CF locations on route-selection. Specifically, CF locations can directly influence drivers' route-selection, then have an impact on the results of the traffic flow assignment model. The obtained traffic flow assignment data are inaccurate without taking into account the impact of CF sites on them. Using the unreliable traffic flow assignment data to evaluate the service ability of CF to be constructed will then influence the rationality of the CF planning results.

In addition, as CF locations can influence the traffic flow distribution, locations of new-built CFs can influence the traffic condition. Consequently, the traffic condition has direct effects on the travel time of EVs. In this sense, the impact of new-built CFs on the traffic condition or the travel time of EVs should be investigated in the CF planning procedure. Unfortunately, papers taking this into account are rare. Many papers including [5]-[7], [11], [12], [14] do not consider the traffic condition in proposed CF planning models. In [8]-[10] [17], the Bureau of Public Roads (BPR) function is used to obtain the travel time of EVs, but the influence of new-built CFs on the traffic condition or the travel time of EVs is ignored. [13] introduces a congestion coefficient of the road section to consider the traffic congestion, but this coefficient is simply set to be a constant value, which is unrealistic. [18] investigates optimal CFs placement considering the congestion caused by EV drivers' charging activities following transportation science research. Nevertheless, the proposed model is discussed in the transportation network but not in a coupled traffic-power system. [19] uses conical congestion function to obtain the travel time of EVs, but ignores the impact of new-built CFs on the travel time of EVs.

To sum up, the relationship between the CF planning model and the traffic assignment model reals that locations of CF can influence the traffic assignment data, while the traffic assignment data also impact CF planning results. After thoroughly reviewing the literature, it has become evident that none of the previous studies incorporated the CF planning model and the traffic assignment model by considering the aforementioned interactions between them.

C. Contributions

Under this background, a Yen's algorithm based CF site planning model in the coupled traffic-power system is proposed in this paper. Compared with published papers, the contributions of this paper are as follows:

1) The proposed CF planning model not only aims to increase the service capacity provided by planned CFs to help EV drivers arrive their destinations within the shortest time at the lowest cost, but also reduce the cost in the power system and the adverse impact of planned CFs on the power system.

2) The traffic assignment model and CF planning model in this work are integrated to obtain the final planning results by considering the interactions between them. More specifically, the CF location planning model influences the traffic assignment data by a novel traffic assignment model based on Yen's algorithm. This traffic assignment model distributes traffic flow considering the impacts of CF locations on route selection by EV drivers. Then, CF planning results are obtained according to the traffic assignment data. It is expected that CF planning results would have the maximum service ability for charging EV and have the least influence on the traffic congestion and the distribution system.

3) The novel traffic assignment model based on Yen's algorithm and locations of candidate CF locations is proposed. Different from many traffic assignment models, which either assume that drivers only choose the shortest path between the origin and destination or ignore the impact of CF sites on the traffic assignment data, the proposed traffic assignment model gives EV driver the chance to take detours to charge his EV in planned CFs and then continue to drive to the destination when the battery energy cannot support EV to reach the destination through the shortest path. In the proposed model, K shortest paths between the origin and the destination are obtained by applying Yen's algorithm. Then drivers choose the shortest path from K paths to reach the destination according to the cruising range and candidate locations of CFs. As a result, the obtained traffic flow assignment data is closer to reality, providing a basis for accurate CF planning results.

4) Different CF planning results will have different impact on route selection by EV drivers and may cause different levels of traffic congestion. Therefore, drive time delay caused by traffic congestion when new CFs are built is taken into consideration in CF planning procedures.

D. Organization of This Paper

The remainder of this paper is organized as follows: Section II illustrates the proposed CF planning model. Section III introduces Yen's algorithm and its application in the proposed traffic flow assignment model. Case studies are given in Section IV. Section V concludes the paper.

II. Charging Facility Planning Model

CF locations not only influence the traffic flow assignment and traffic congestion in the TS but also affect the stability and economic efficiency of DS directly. Therefore, the CF planning model is developed to obtain an optimal CF planning scheme for both TS and DS. The objective function can be formulated as

$$\min F = F_T + F_E \tag{1}$$

The objective function (1) is to minimize the overall EV transportation cost in TS, F_T, and the operation cost in DS, F_E. Detail formulations of F_T and F_E are given as follows.

A. Minimizing Transportation Cost

In TS, the optimal CF planning aims to help EV drivers arrive their destinations within the shortest time at the lowest cost.

Therefore, the transportation cost consists of three components, namely travel time cost, delay cost and travel failure cost, which can be expressed as

$$F_T = f_{tra} + f_{del} + f_{fail} \tag{2}$$

The overall travel time cost f_{tra} can be calculated according to (3), which is determined by the time spend to complete the trip.

$$f_{tra} = c^{tra} \sum_{\tau \in \Omega^T} \sum_{(rs) \in \Omega^{PT}} f_\tau^{rs} T_{rs,\tau}^{tra} \gamma_\tau^{rs} \tag{3}$$

where

$$T_{rs,\tau}^{tra} = \sum_{l \in \Omega^{LT}} T_l^{rs,\tau} + \sum_{h \in \Omega^H} T_h^{rs,ch} \varphi_h^{rs}, \forall (rs) \in \Omega^{PT}, \forall \tau \in \Omega^T, \forall h \in \Omega^H \tag{4}$$

$$T_l^{rs,\tau} = T_l^0 \left[1 + 0.15 \left(\frac{x_{l,t}}{cap_l} \right)^4 \right], \forall l \in \Omega^{LT} \tag{5}$$

$$x_{l,t} = \sum_{(rs) \in \Omega^{PT}} \sum_{\tau \in \Omega^T} f_\tau^{rs} \delta_l^{rs}, \forall t \in \Omega^T, \forall l \in \Omega^{LT} \tag{6}$$

$$T_h^{rs,ch} = \frac{EC^{EV} L}{p^{EV}}, \quad \forall h \in \Omega^H \tag{7}$$

It is possible for drivers to drive from the origin node to the destination node by following a path (or a route) through the transportation network. Each path is a sequence of directed links leading from one node to another [20]. It is assumed that if an EV has no available path to complete the trip, the driver will not drive the car on the road but stay at the origin node. In (3), f_τ^{rs} represents the EV flow generated at time τ by the travel demand from the origin node r to the destination node s; γ_τ^{rs} is a binary variable which denotes whether or not the EV flow can complete its trip (arrive at the destination); and $T_{rs,\tau}^{tra}$ is the travel time of EV flow, f_τ^{rs}. Equations (4)-(7) give the mathematical definitions of $T_{rs,\tau}^{tra}$. The travel time of EV flow is composed of two parts: driving time on roads and charging time at CFs as shown in (4). The driving time is determined by the length of selected links and also affected by traffic volumes of links in time t. Driving time on path rs includes the time consumption on each link EV flow passed through, which is formulated as (5) [21]. It is an increasing sequence, which is called Bureau of Public Roads (BPR) function; T_l^0 is the free travel time across link l (i.e. travel time across link l at the speed limit without causing congestion); $x_{l,t}$ represents the sum of EV flow on link l at time t, the mathematical definition of which is shown in (6); and cap_l is the capacity of link l. Therefore, the driving time of each EV increases as the traffic flow on the road increases. The traffic congestion will cause the increase of the travel time. Then the overall travel time cost f_{tra} increases and influences the value of the objective function. The second part in (4) is the overall charging time, where $T_h^{rs,ch}$ is calculated by (7), and φ_h^{rs} is a binary variable which represents whether or not EVs on path rs are charged at candidate CF h; L is the distance between node r to the first CF or the distance between two adjacent CFs; and EC^{EV} is EV power consumption per mile.

To help EV drivers complete their trips as soon as possible, the total delay cost caused by the traffic congestion is considered separately and implies an additional penalty for the traffic congestion which may be caused by newly-built CFs, as shown in (8). Also, (9) presents the delay time $T_{rs,\tau}^{del}$ of each EV flow, which is the difference between actual travel time $T_{rs,\tau}^{tra}$ and free travel time T_{rs}^0. The mathematical definition of T_{rs}^0 is given in (10).

$$f_{del} = c^{del} \sum_{\tau \in \Omega^T} \sum_{(rs) \in \Omega^{PT}} f_\tau^{rs} T_{rs,\tau}^{del} \gamma_\tau^{rs} \tag{8}$$

$$T_{rs,\tau}^{del} = T_{rs,\tau}^{tra} - T_{rs}^0, \forall (rs) \in \Omega^{PT}, \forall \tau \in \Omega^T \tag{9}$$

$$T_{rs}^0 = \sum_{l \in \Omega^{LT}} T_l^0 \delta_l^{rs} + \sum_{h \in \Omega^H} T_h^{rs,ch} \varphi_h^{rs}, \forall (rs) \in \Omega^{PT}, \forall h \in \Omega^H \tag{10}$$

For all EV flows, the main concern is to complete trips. If the EV battery capacity is insufficient for the whole trip, EV cannot arrive at the destination without charging the battery on the way. Therefore, a penalty cost for failing to arrive at destinations is added as part of the total cost of the TS as

$$f_{fail} = c^{fail} \sum_{\tau \in \Omega^T} \sum_{(rs) \in \Omega^{PT}} f_\tau^{rs} (1 - \gamma_\tau^{rs}) \tag{11}$$

B. Minimizing Distribution System (DS) Operation Cost

The locations of CFs also have an impact on the operation cost of the DS. Three components are taken into consideration: generation cost, penalty cost for voltage deviation and power loss. Therefore, the DS operation cost is described as

$$F_E = f_{gen} + f_{vd} + f_{pl} \tag{12}$$

The detailed calculation of generation cost f_{gen} is given in (13) to (20). Eq. (14) represents the piecewise linear generation cost function. Eq. (15) is the multi-period power flow equality constraint. In (16), the CF power is composed of the power consumed by FCSs and BSSs; u_i^F and u_i^B are variable decisions for FCS and BSS on node i, respectively. Equation (17) denotes that the active power of FCS at time t is determined by the number of EVs. Equation (18) explains how to calculate the average active power of BSSs. The proposed traffic assignment model to be introduced in Section III is to assign the EV flow from origin r to destination s which starts travel at time τ, f_τ^{rs} and obtain the EV flow from origin r to destination s on node i at time t, $f_{i,t}^{rs}$. The relationship between f_τ^{rs} and $f_{i,t}^{rs}$ is shown in equation (19). In equation (19), φ_h^{rs} is the binary decision variable for whether EV flow f_τ^{rs} has charged at the hth candidate CF. And γ_τ^{rs} is the binary decision variable for whether the EV flow f_τ^{rs} could complete its trip.

$$f_{gen} = \sum_{i \in \Omega^{ND}} \sum_{t \in \Omega^T} C_{i,t}^{GEN} \tag{13}$$

$$C_{i,t}^{GEN} = \begin{cases} a_{1,i} \times P_{i,t}^{GEN} + z_{1,i}, & P_{i,t}^{GEN} \le P_{x1} \\ a_{2,i} \times P_{i,t}^{GEN} + z_{2,i}, & P_{x1} < P_{i,t}^{GEN} \le P_{x2} \\ \vdots & \vdots \\ a_{n,i} \times P_{i,t}^{GEN} + z_{n,i}, & P_{xn-1} < P_{i,t}^{GEN} \le P_{xn} \end{cases}, \quad \forall P_{xn} \in \Omega^{GP}, \forall t \in \Omega^T, \forall i \in \Omega^{ND}, \quad \forall a_{n,i} \in \Omega^A, \forall z_{n,i} \in \Omega^Z \tag{14}$$

$$P_{i,t}^{GEN} = P_{i,t}^D + P_{i,t}^{CF} + U_{i,t} \sum_{i,j \in \Omega^{ND}} U_{j,t} \left(G_{ij} \cos \theta_{ij,t} + B_{ij} \sin \theta_{ij,t} \right) \quad \forall t \in \Omega^T, \forall i, j \in \Omega^{ND} \tag{15}$$

$$P_{i,t}^{CF} = u_i^F P_{i,t}^{FCS} + u_i^B P_{i,t}^{BSS}, \forall t \in \Omega^T, \forall i \in \Omega^{ND} \tag{16}$$

$$P_{i,t}^{FCS} = p^{EV} \sum_{(rs) \in \Omega^{PT}} f_{i,t}^{rs}, \forall t \in \Omega^T, \forall i \in \Omega^{ND} \tag{17}$$

$$P_{i,t}^{BSS} = p^{EV} \sum_{t\in\Omega^T} \sum_{(rs)\in\Omega^{PT}} f_{i,t}^{rs} / T, \forall t \in \Omega^T, \forall i \in \Omega^{ND} \quad (18)$$

$$f_{i,t}^{rs} = \varphi_h^{rs} \gamma_\tau^{rs} f_\tau^{rs} \quad (19)$$

The second component is to limit the voltage deviation after constructing CFs to maintain the safe operation of DS. To minimize the voltage deviation, it can be expressed as the total penalty cost for absolute deviations in voltage magnitudes on DS nodes [22]:

$$f_{vd} = c^{VD} \sum_{i\in\Omega^{ND}} \sum_{t\in\Omega^T} \left| U_{i,t} - U_{i,rating} \right| \quad (20)$$

where $U_{i,rating}$ corresponds to the rated voltage on node i that can be set to 1 p.u.

At last, power loss cost can be expressed as

$$f_{pl} = c^{pl} \sum_{(ij)\in\Omega^{LD}} \sum_{t\in\Omega^T} \left[G_{ij} \left(U_{i,t}^2 + U_{j,t}^2 - 2U_{i,t}U_{j,t} \cos\theta_{ij,t} \right) \right] \quad \forall i, j \in \Omega^{ND} \quad (21)$$

C. *Constraints*

The constraints are formulated as follows:

Subject to

1) Active power limit of generators

$$\left(P_{i,t}^{GEN}\right)^2 + \left(Q_{i,t}^{GEN}\right)^2 \le \left(S_{i,\max}^{GEN}\right)^2, \forall t \in \Omega^T, \forall i, j \in \Omega^{ND} \quad (22)$$

2) Electricity branch flow limit

$$P_{ij,t} = U_{i,t}^2 G_{ij} + U_{i,t}U_{j,t} \left(G_{ij} \cos\theta_{ij,t} + B_{ij} \sin\theta_{ij,t} \right) \quad \forall t \in \Omega^T, \forall (ij) \in \Omega^{LD} \quad (23)$$

$$Q_{ij,t} = -U_{i,t}^2 B_{ij} - U_{i,t}U_{j,t} \left(G_{ij} \cos\theta_{ij,t} + B_{ij} \sin\theta_{ij,t} \right) \quad \forall t \in \Omega^T, \forall (ij) \in \Omega^{LD} \quad (24)$$

$$P_{ij,t}^2 + Q_{ij,t}^2 \le \left(S_{ij}^{\max}\right)^2, \forall t \in \Omega^T, \forall i, j \in \Omega^{ND} \quad (25)$$

3) Nodal voltage limit

$$U_i^{\min} \le U_{i,t} \le U_i^{\max}, \forall t \in \Omega^T, \forall i \in \Omega^{ND} \quad (26)$$

4) CF number constraints

$$\sum_{i\in\Omega^{ND}} u_i^F = N^F \quad (27)$$

$$\sum_{i\in\Omega^{ND}} u_i^B = N^B \quad (28)$$

III. YEN'S ALGORITHM AND ROUTE SELECTION

A. Description of Yen's Algorithm

TABLE I
PSEUDOCODE TO OBTAIN *K*-SHORTEST PATHS

Algorithm: searching *K*-shortest paths

function Yen's Algorithm (*Graph, origin, destination, K*)
  initialize *A* and *B*
  A^1 = the shortest path from the origin to the destination
  for(1) every *k* (*k*>1) **in** *K* **do**
    for(2) every *q* **in** A^{k-1} without destination **do**
      spurNode = *q*;
      rootPath = A^{k-1} from *origin* to *spurNode*;
      for(3) each *path p* **in** *A* **do**
        if *rootPath* equals to links *p*. (the origin, *q*) **do**
          remove edge p.(*spurNode*, *spurNode* +1) from *Graph*;
        end if
      end for(3)
      for(4) each *rootPathNode* in *rootPath* except *spurNode*
        remove *rootPathNode* from *Graph*;
      end for(4)
      spurPath = the shortest path from node *q* to the destination
      A_q^k = *rootPath* + *spurPath*
      Save A_q^k in *B*
      restore *edges* to *Graph*;
      restore *nodes* in *rootPath* to *Graph*
    end for(2)
    if *B* is empty
      break
    end if
    A^k = the shortest path of *B*
  end for(1)

Yen's algorithm, proposed in [23], provides a method to find *K* shortest loopless paths from one point to another in a network. It can only be applied to an acyclic network where weights are positive between any two points. According to this algorithm, EV drivers have *K* potential paths at most to reach the destination considering the cruising range.

TABLE II
PSEUDOCODE TO THE PROPOSED TRAFFIC ASSIGNMENT MODEL

Algorithm 2: Route selection

Generate candidate FCSs and BSSs;
for(1) every charging or battery swapping type EV flow **do**
  Generate *K* shortest-paths by *Algorithm* 1;
  Set *k*=1;
  while(2) (*k* <= *K*) **do**
    if R_{veh} is longer than the length of A^k **then**
      ① $\delta_l^{rs} = 1, \gamma_\tau^{rs} = 1, \varphi_h^{rs} = 0$;
      Leave **while(2)** and return to **for(1)** to move to next EV flow;
    else if no appropriate type CF is on A^k **then**
      ② $\delta_l^{rs} = 0, \gamma_\tau^{rs} = 0, \varphi_h^{rs} = 0$;
      Set *k*=*k*+1;
    else if the EV flow arrives at the destination node after charging at CFs **then**
      ③ $\delta_l^{rs} = 1, \gamma_\tau^{rs} = 1, \varphi_h^{rs} = 1$;
      Leave **while(2)** and return to **for(1)** to move to next EV flow;
    else
      ④ $\delta_l^{rs} = 0, \gamma_\tau^{rs} = 0, \varphi_h^{rs} = 0$;
      Set *k*=*k*+1;
    end if
  end while(2)
  if there is no optional path for the EV flow **then**
    ⑤ $\delta_l^{rs} = 0, \gamma_\tau^{rs} = 0, \varphi_h^{rs} = 0$;
  end if
end for(1)

A transportation network is a weighted directed graph. In the Yen's algorithm, K shortest paths can be found by K iterations, which are stored in set A. In the first iteration, the shortest path A^1 in a network is found by any efficient shortest path algorithm, then the second shortest path A^2,… , the K shortest path A^K is selected. Before determining the k shortest path A^k (k>1), each node on the last shortest path A^{k-1} (except the destination) is selected as a *deviation node* q. Potential shortest paths are found to select A^k. Each potential shortest path consists of a rootpath and a spurpath. The rootpath is the subpath from the origin to node q in A^{k-1}. If A^j (j=1,…, k-1) has the same rootpath, remove the link between node q and q+1 in A^j from the graph. Then, remove nodes on rootpath (except the deviation node) from the graph. The spurpath is selected as the shortest path from node q to the destination in the graph. For each deviation node, there is a potential shortest path. Finally, the shortest one of all the potential paths is determined as A^k. The pseudocode of Yen's algorithm to search K shortest loopless paths is illustrated in Table I.

B. A Novel Traffic flow Assignment Model

The proposed traffic flow assignment model is based on Yen's algorithm and locations of candidate CFs, which aims to obtain the traffic flow assignment data, $f_{i,t}^{rs}$ mentioned in (17)-(19). In section III. A, K paths (A^1 to A^K) have been found for each origin-destination (O-D) pair, and the lengths of these paths are incremental. According to the remaining battery energy, EV drivers hope to choose the path as short as possible. Paths are tested one by one from A^1 to A^K until EV drivers can complete their trips through the tested path. It means that the shortest path through which drivers can complete their trip is the selected path. Basing on the aforementioned route selection method, the traffic flow assignment data ($f_{i,t}^{rs}$) can be obtained. The specific process for this traffic flow assignment model is shown in Table II. From situation ① in Table II , it can be seen that if the length of tested path A^k is less than or equal to EV's cruising range R_{veh}, the path is the selected path. In this situation, EVs can complete the trip without charging, leading to $\gamma_\tau^{rs}=1$, $\delta_l^{rs}=1(l\in A^k)$, and $\varphi_h^{rs}=0$. If R_{veh} is less than the length, EVs must be charged to complete the trip. As seen in Table II (situations ②-④), three conditions must be satisfied to select the test path: 1) there is at least one appropriate type of CF on the path; 2) the remaining battery energy can support EVs to reach the CFs, 3) after each charging, the EVs can reach the next CF, and eventually arrive at the destination. Situation ⑤ in Table II means that EVs have tried all the K paths, but still cannot find a path to reach the destination. This is because the R_{veh} is too short, or the number of CFs is not enough or the locations of CFs are unreasonable. These EVs that cannot arrive at destinations will incur a travel failure cost as depicted in (11).

IV. Case Studies

A. Experiment Setting

The proposed model is validated on a coupled 25-node transportation and 30-node DS, as depicted in Fig. 1. The detailed link lengths of the TS are available in [24]. The capacities and design speeds of roads are consistent with the characteristics of the main roads in China [25]. The topology of 30-node DS can be found in case30pwl from MATPOWER with a triple transmission capacity. O-D pairs and traffic flow are randomly generated, and the number of EVs for each O-D pair is set as 4-6 per hour. It is assumed that there are 600 O-D pairs and 50,000 EVs, containing fast-charging cars and battery-swapping cars. The time interval is set to 10 minutes. Queue time t_q in (18) is assumed to be one time interval (10 minutes). Table III lists some crucial parameters. It is assumed that 3 FCSs and 3 BSSs will be constructed. There are 6 candidate locations both for FCSs and BSSs, as given in Table IV. This case simulates the operation of the system for 24 hours in a day. It is assumed that before departure, the EV battery is fully charged.

B. Results and Discussion

a) Case 1: compare with CF planning results based on other traffic flow assignment model

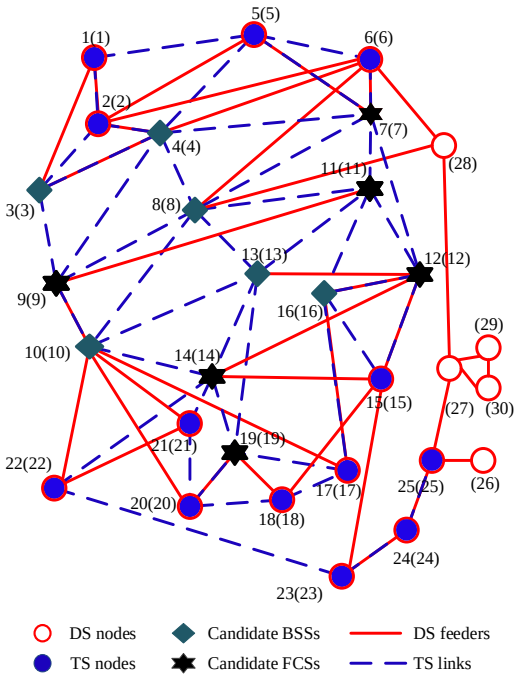

Fig. 1 Test system coupled DS and TS

TABLE III
SETTINGS OF SOME CRUCIAL PARAMETERS

Parameters	c^{tra}	c^{del}	c^{fail}	c^{vd}	c^{pl}
Value	0.5 ($/10min)	1.5 ($/10min)	187.5 ($/veh)	1500 ($)	50 ($/MW)

TABLE IV
LOCATIONS FOR CANDIDATE FCSS AND BSSS

CF Type	Locations					
FCS	3	4	8	10	13	16
BSS	7	9	11	12	14	19

TABLE V
CF PLANNING RESULTS OF DIFFERENT MODELS

	FCS			BSS		
A	8	10	13	7	12	14
B	4	10	13	9	11	14

A: Comparison model; B: Proposed model.

TABLE VI
DETAILED FINANCIAL INDICATORS OF DIFFERENT MODELS ($10^5$$)

A	F = **49.73**	
	F_T = 34.19	F_E = 15.54

	f_{tra}	f_{del}	f_{fail}	f_{gen}	f_{VD}	f_{pl}
	4.58	1.21	**28.40**	10.52	4.859	0.168
B	F = **40.45**					
	F_T = 23.99			F_E = 16.47		
	f_{tra}	f_{del}	f_{fail}	f_{gen}	f_{VD}	f_{pl}
	6.48	2.09	**15.42**	11.42	4.862	0.185

A: Comparison model; B: Proposed model.

To prove the merits of the proposed traffic flow assignment model based on Yen's algorithm, this case compares the results of CF planning model coupled with the proposed traffic flow assignment model with those coupled with other traffic flow assignment models mentioned in previously published papers. The traffic flow assignment models in [5] and [6] are similar and all assume that traffic flow is distributed to the shortest path between the origin and the destination. If the battery capacity cannot support EVs to reach the destination through the shortest path because there are not enough CFs on this path, it is assumed that the trip fails. This means that EV drivers have no other choices when they cannot arrive at the destination through this shortest path, which is unrealistic. Actually, when the battery capacity is not enough for the shortest route, drivers are willing to take detours to charge EV in order to complete the trip. The CF planning model coupled with these two similar traffic flow assignment models is regarded as the comparison model.

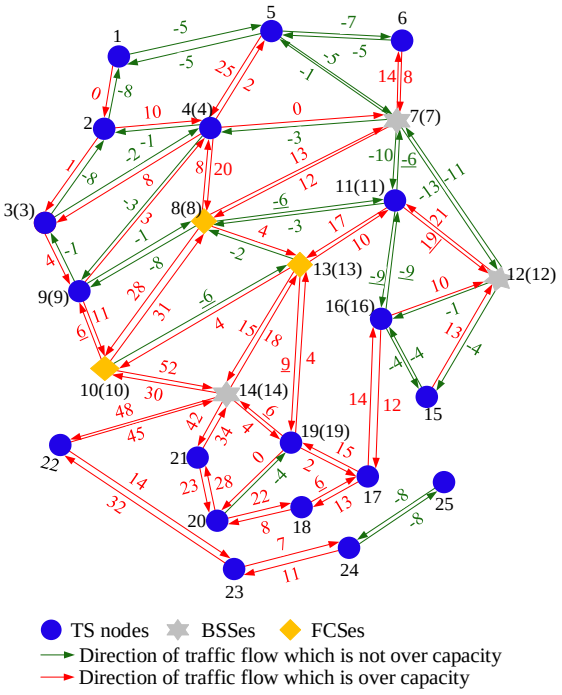

Fig. 2 The difference between the EV flow in rush hour and road capacity in the comparison CF planning model

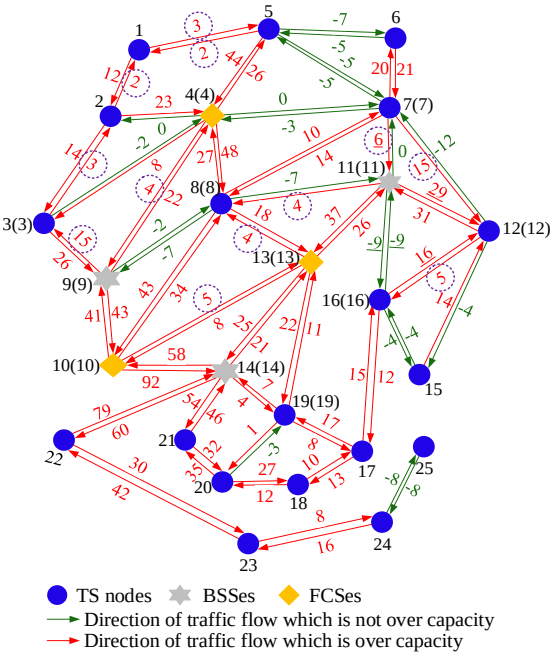

Fig. 3 The difference between the EV flow in rush hour and road capacity in the proposed CF planning model

In the proposed model, K is set to 10. In this situation, EVs have 10 options to travel and can select the most suitable path from 10 possible options. The cruising range of all EVs is set at 250 km, which is derived from BYD EV500 with a range of 500km. To ensure that EVs can return to origins after arriving at destinations, the cruising range is set as half value of the actual cruising range.

Tables V and VI respectively show the CF planning results and detailed financial indicators in different models. It can be found that the planning results are different. Specifically, the overall cost, as well as the failure cost in the comparison model, are larger than that in the proposed model. This is because in the comparison mode if an EV cannot arrive at the destination via the shortest path, the travel fails. But in the proposed model, because EV drivers have more options to arrive at the destination, the possibility to complete the trip is higher. The number of EVs which cannot complete their trips in the comparison model (named failed EVs) is about twice as in the proposed model, which is given by Table VII.

TABLE VII
THE NUMBER OF FAILED EVS

	The number of failed EVs
A	15146
B	8222

The traffic flow distributions in the two models are illustrated in Figs. 2 and 3, respectively. The difference between the maximum traffic flow (8:50 am-9:00 am) in a day and the road capacity in a time interval (10 minutes) is illustrated in these two figures. Green numbers and arrows indicate that the traffic flow is not more than road capacity, and red ones indicate that the traffic flow is greater than the road capacity. The purple circle means newly added congested road in the proposed model compared with the comparison model. It is seen from Fig. 3 that 12 more congested roads are newly added in the proposed model. As shown in Table VII, there are 6924 more EVs on the road in the proposed model. Therefore, in rush hour, roads are

more crowded in the proposed model. Moreover, the congestion of links connecting CFs is severer in the proposed model. This is because when EVs fail to travel via the shortest path as the EV battery power is limited, they look for other longer paths to pass CFs to complete the trip.

TABLE VIII
PLANNING RESULTS WITH DIFFERENT K

K	CF locations						$F(10^6\$)$
	FCS			BSS			
1	8	10	13	7	12	14	4.97
2	4	10	13	7	9	14	4.55
3	**4**	**10**	**13**	**9**	**11**	**14**	**4.34**
4	4	10	13	9	11	14	4.27
5	4	10	13	9	11	14	4.17
6	4	10	13	9	11	14	4.15
7	4	10	13	9	11	14	4.13
8	4	10	13	9	11	14	4.08
9	4	10	13	9	11	14	4.05
10	4	10	13	9	11	14	4.05
100	4	10	13	9	11	14	**3.91**

b) Case 2: CFs' planning results with different K

This case investigates the influence of K's value on the planning result. In this case, the cruising range is also set at 250km. The CF planning results and overall costs with K from 1 to 10 are given in Table VIII. It can be seen that as K's value increases, the total cost decreases. The planning results remain stable since K=3.

Table IX shows details of F_T and F_E with different K respectively. As observed, as K increases, F_T decreases and the general trend for F_E increases slightly. At the same time, f_{fail} (the failure cost) reduces when K increases. This proves that as K increases, more EVs can arrive destinations. The numbers of EVs which fail to complete their trips with different K (failed EV) are displayed in Fig. 4. It can be observed from Fig. 4 that the number of failed EVs decreases as K increases, which further validates the aforementioned conclusions.

TABLE IX
DETAILS OF F_T AND F_E WITH DIFFERENT K (10^5\$)

K	f_{tra}	f_{del}	f_{fail}	F_T	f_{gen}	f_{pl}	f_{VD}	F_E
1	4.58	1.21	28.40	34.19	10.52	0.168	4.86	15.54
2	5.58	1.82	22.02	29.41	11.07	0.179	4.86	16.11
3	5.67	1.46	20.27	27.40	10.95	0.176	4.85	15.97
4	5.94	1.75	18.90	26.58	11.11	0.179	4.85	16.14
5	6.08	1.70	17.65	25.43	11.23	0.182	4.85	16.26
6	6.14	1.77	17.30	25.21	11.26	0.182	4.86	16.30
7	6.19	1.80	16.98	24.97	11.30	0.183	4.86	16.34
8	6.34	1.93	16.12	24.39	11.37	0.184	4.86	16.41
9	6.45	2.05	15.53	24.04	11.40	0.185	4.86	16.45
10	6.48	2.09	15.42	23.99	11.42	0.185	4.86	16.47

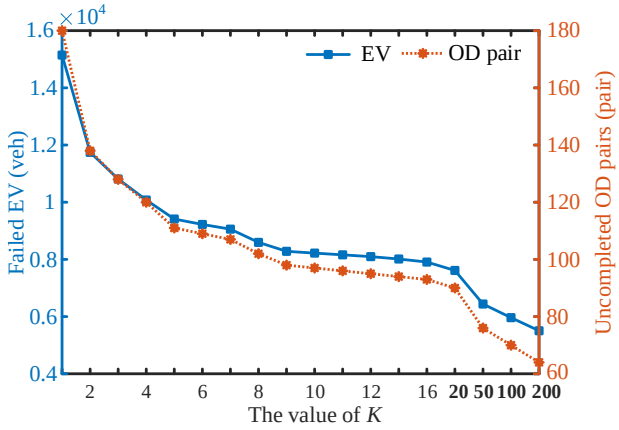

Fig. 4 Numbers of failed EVs and uncompleted O-D pairs with different K.

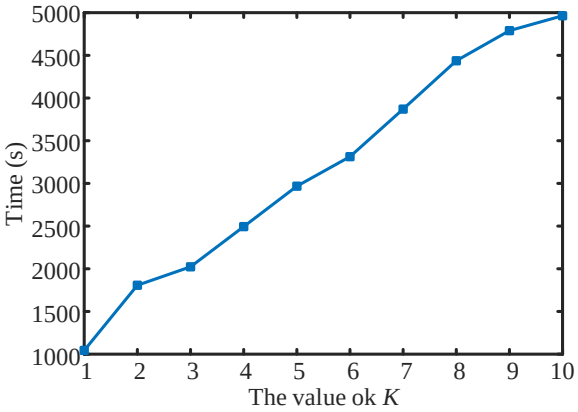

Fig. 5 Computing time with different K

As there are more EVs traveling on the roads, both the transportation cost f_{tra} and delay cost f_{del} grow, which is also shown in Table IX. The slight growth of F_E can be explained by the growing number of EVs charged by CFs. Because the reduction of the failure cost is larger than the increased margin of other costs, the overall cost decreases. Further, in Fig. 4, the rate of decrease of failed EV number slows down when K is larger than 9. Since the most suitable path for the same O-D pair is the same, the number of O-D pair which cannot complete the trip is relevant to the number of failed EVs. The change curve of the number of uncompleted O-D pair depicted in Fig. 4 shows that the uncompleted OD pair decreases as K increases and the rate of decrease of uncompleted O-D pair number slows down since K=9. When K increases from 100 to 200, only six more O-D pairs are completed. The computing time with different K from 1 to 10 is illustrated in Fig. 5. When K equals to 100, the computing time is 66627 s (18.5 hours). Therefore, setting a large value to K is not worth with too long computing time and limited arrival rate improvement. In realistic application, a suitable value of K is needed as CF plan will not change with the growth of K and the computing time should be acceptable.

c) Case 3: the impact of c^{fail} on planning results

This case aims to investigate the impact of c^{fail} on the CF planning results. In this case, K is set at 20. Table X shows the planning results of FCSs and BSSs with different c^{fail}. It reveals that as c^{fail} increases, the number of failed EV decreases rapidly and remains constant since c^{fail} is larger than 112.5. And since

c^{fail} is larger than 112.5, the planning results remains unchanged at FCS:{4, 10, 13} and BSS :{9, 11, 14}.

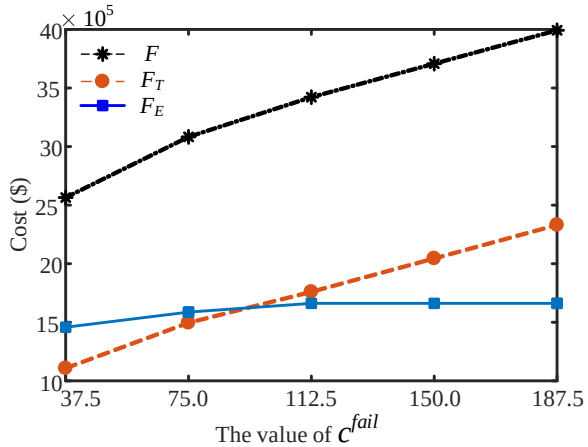

Fig. 6 F, F_E and F_T with different c^{fail}

TABLE X
PLANNING RESULTS WITH DIFFERENT FAILURE COST

c^{fail}	FCS			BSS			Failed EV
37.5	3	4	8	9	12	19	20173
75.0	3	10	13	7	12	11	12121
112.5	10	4	13	9	11	14	7614
150.0	10	4	13	9	11	14	7614
187.5	10	4	13	9	11	14	7614

TABLE XI
THE CRUISING RANGES OF COMMON EVS ON THE MARKET

EV Types	R_{veh} (km)	EV Types	R_{veh} (km)
BYD Song EV500	500	BYD Yuan EV360	360
BYD Qin EV450	480	ROEWE ERX5	320
BAIC BJEV New Energy EU400	460	ZD D3	210
BAIC BJEV New Energy EU5	416	ZD D2s	180

TABLE XII
LOCATIONS OF CFS AND COSTS WITH DIFFERENT CRUISING RANGE

R_{veh} (km)	CF locations						F(10^6\$)	Failed EVs (veh)
	FCS			BSS				
500	4	10	13	9	11	14	4.05	8222
480	4	10	13	9	11	14	4.05	8222
460	8	10	13	9	11	14	4.30	10246
416	8	10	13	7	11	14	4.51	10799
360	8	10	13	9	19	14	5.67	19266
320	4	8	10	11	14	19	6.77	26027
210	3	4	13	12	14	19	9.45	42764
180	3	4	13	11	12	14	9.76	44550

Fig. 6 illustrates the value of F, F_E and F_T with different c^{fail}. We can see that F_T and F increase as c^{fail} increases. When c^{fail} is larger than 112.5, F_E remains unchanged. Figs. 7 and 8 illustrate detailed financial indicators of F_T and F_E with different c^{fail}. It can be seen that when c^{fail} is large than 112.5, all detailed financial indicators of F_T and F_E are unchanged except f^{fail}. This is because when c^{fail} is large enough, the CF construction plan and the number of EVs charged by CFs do not change. It can be concluded that in proposed model a sufficient value of c^{fail} is needed. When the value of c^{fail} is not adequate (i.e. less than 112.5), obtained CF planning results are unstable and planned CFs cannot serve enough EVs as more than 24 % EVs cannot arrive their destinations.

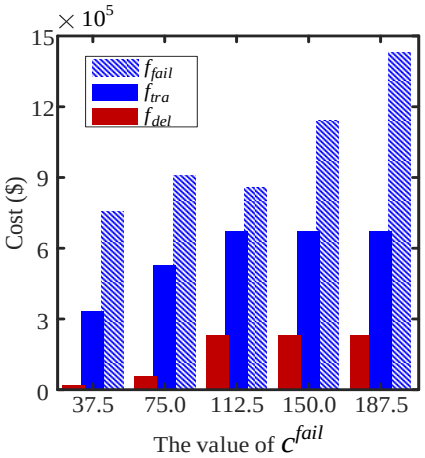

Fig. 7 Details of F_T with different c^{fail}

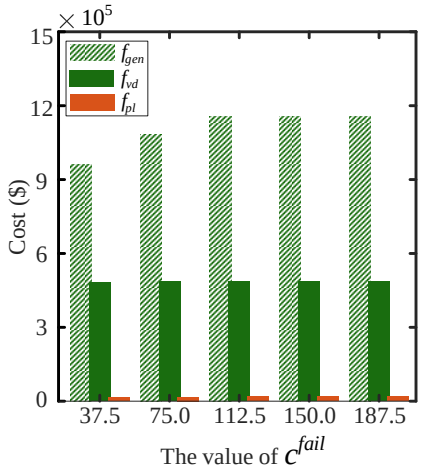

Fig. 8 Details of F_E with different c^{fail}

d) Case 4: the influence of cruising range on planning results

This section examines the impact of EV cruising range R_{veh} on planning results. The cruising ranges of various EVs on the market are listed in Table XI, which are used to investigate the influence of EV cruising range R_{veh} on planning results in this case. When K is set at 10, and c^{fail} is set at 187.5 (\$/veh).

TABLE XIII
F_E AND F_T COST DETAILS (10^5\$) WITH DIFFERENT CRUISING RANGE

R_{veh} (km)	f_{tra}	f_{del}	f_{fail}	F_T	f_{gen}	f_{pl}	f_{VD}	F_E
500	6.48	2.09	15.42	23.99	11.42	0.185	4.86	16.46
480	6.48	2.09	15.42	24.15	11.42	0.185	4.86	16.47
460	5.93	1.22	19.21	26.26	11.69	0.194	4.87	16.75
416	5.90	1.56	20.25	27.71	12.3	0.204	4.88	17.38
360	3.93	0.49	36.12	40.54	11.15	0.185	4.87	16.20
320	2.80	0.14	48.8	51.74	10.96	0.182	4.84	15.98
210	0.39	0	80.18	80.57	9.00	0.136	4.78	13.91
180	0.25	0	83.53	83.78	8.90	0.132	4.77	13.80

Tables XII and XIII show the results with different R_{veh}. According to Table XII, cruising range has obvious influence on planning results. If the cruising range is small, the overall cost will be high and the number of failed EVs will be large. When R_{veh} =180 km (the lowest value in Table XII), the overall cost exceeds 9×10^6\$, and about 89.1% of EVs cannot arrive destinations. It should be noted that there are other types of EVs for sale which have shorter cruising range than 180 km. With the reduction of R_{veh}, the number of failed EVs increases rapidly, and F_E decreases due to the reduced charging load, as shown in

Tables XII and XIII. When R_{veh} is less than 210 km, there is no more congestion in the TS and f_{del} is zero, which can be seen in Table XIII. This is because there are very few EVs on the road in this situation. The results indicate that for this coupled system, if the EV cruising range is not sufficient, more new CFs are needed to be planned to help EVs to complete their trips.

V. Conclusion

A novel CF planning model for the coupled electric-traffic network basing on Yen's algorithm is proposed in this paper. In this model, the impacts of planned CFs on both TS and DS are considered simultaneously. Simulation results show that the CF planning results of the proposed model can charge more EVs and help more EVs to arrive destinations while considering the impacts of CFs on EV flow assignment and road congestion. This model can obtain optimal CF planning results for both TS and DS. Also, suitable values of two parameters (i.e. K and c^{fail}) in the proposed model will help improve its accuracy.

References

[1] J. Hu, Z. Li, J. Zhu, and J. M. Guerrero, "Voltage stabilization: a critical step toward high photovoltaic penetration," *IEEE Ind. Electron. Mag*, vol. 13, no. 2, pp. 17-30, June 2019.

[2] A. G. Boulanger, A. C. Chu, S. Maxx and D. L. Waltz, "Vehicle electrification: status and issues," *Proceedings of the IEEE*, vol. 99, no. 6, pp. 1116-1138, Jun. 2011.

[3] W. Sierzchula, S. Bakker, K. Maat and B. V. Wee, "The influence of financial incentives and other socio-economic factors on electric vehicle adoption," *Energy Polcy*, vol. 68, pp. 183-194, 2014.

[4] W. Wei, S. Mei, L. Wu, M. Shahidehpour, Y. Fang, "Optimal Traffic-Power Flow in Urban Electrified Transportation Networks," *IEEE Transactions on Smart Grid*, vol. 8, no. 1, pp. 84-95. 2017.

[5] G. Wang, Z. Xu, F. Wen and K. P. Wong, "Traffic-Constrained Multiobjective Planning of Electric-Vehicle Charging Stations," *IEEE Transactions on Power Delivery*, vol. 28, no. 4, pp. 2363-2372, Oct. 2013.

[6] G. Wang, X. Zhang, H. Wang, J. Peng, H. Jiang, Y. Liu, C. Wu, Z. Xu, W. Liu, "Robust Planning of Electric Vehicle Charging Facilities with Advanced Evaluation Method," *IEEE Trans. Ind. Informat.*, vol. 14, no. 1, pp. 321-331, Jan. 2018.

[7] X. Huang, J. Chen, H. Yang, Y. Cao, W. Guan and B. Huang, "Economic planning approach for electric vehicle charging stations integrating traffic and power grid constraints," *IET Generation, Transmission & Distribution*, vol. 12, no. 17, pp. 3925-3934, Sep. 2018.

[8] W. Yao, J. Zhao, F. Wen, Z. Dong, Y. Xue, Y. Xu, and K. Meng, "A multi-objective collaborative planning strategy for integrated power distribution and EV charging systems," *IEEE Trans. Power Syst.*, vol. 29, no.4, pp. 1811-1821, Jul. 2014.

[9] Y. Xiang, J. Liu, R. Li, F. Li, C. Gu, S. Tang, "Economic planning of electric vehicle charging stations considering traffic constraints and load profile templates," *Appl. Energy*, vol. 178, pp. 647–659. Sep. 2016.

[10] X. Wang, M. Shahidehpour, C. Jiang and Z. Li, "Coordinated Planning Strategy for Electric Vehicle Charging Stations and Coupled Traffic-Electric Networks," *IEEE Transactions on Power Systems*, vol. 34, no. 1, pp. 268-279, Jan. 2019.

[11] Zhang, H., Moura, S.J., Hu, Z. and Song, Y., 2016. PEV fast-charging station siting and sizing on coupled transportation and power networks. IEEE Transactions on Smart Grid, 9(4), pp.2595-2605.

[12] Shukla, A., Verma, K. and Kumar, R., 2019. Multi-objective synergistic planning of EV fast-charging stations in the distribution system coupled with the transportation network. IET Generation, Transmission & Distribution, 13(15), pp.3421-3432.

[13] Xiang, L.I., LI, Q.G., WANG, H.L. and ZHU, N.H., 2018. Planning of Fast Charging Stations Considering Distribution Grid and Transportation Network. DEStech Transactions on Environment, Energy and Earth Sciences, (epeee).

[14] Mao, D., Wang, J., Tan, J., Liu, G., Xu, Y. and Li, J., 2019, June. Location Planning of Fast Charging Station considering its Impact on the Power Grid Assets. In 2019 IEEE Transportation Electrification Conference and Expo (ITEC) (pp. 1-5). IEEE.

[15] Fuchun Shao. *Transportation planning*. China: China railway publishing house Press, 2016.

[16] N. Shahraki, H. Cai, M. Turkay, and M. Xu, "Optimal locations of electric public charging stations using real world vehicle travel patterns," *Transp. Res. D, Tr. E.*, vol. 41, pp. 165 – 176, Dec. 2015.

[17] He F , Yin Y , Wang J , et al. Sustainability SI: Optimal Prices of Electricity at Public Charging Stations for Plug-in Electric Vehicles. Networks and Spatial Economics, 2016, 16(1):131-154.

[18] Xiong Y , Gan J , An B , et al. Optimal Electric Vehicle Fast Charging Station Placement Based on Game Theoretical Framework[J]. IEEE Transactions on Intelligent Transportation Systems, 2017:1-12.

[19] Wang S , Dong Z Y , Luo F , et al. Stochastic Collaborative Planning of Electric Vehicle Charging Stations and Power Distribution System. IEEE Transactions on Industrial Informatics, vol.14,no. 1,pp. 321- 331.Jan. 2018.

[20] Yosef Sheffi, "Urban Transportation networks: Equilibrium analysis with mathmatial programing methods", Prentice Hall, Jan.1985.

[21] Traffic Assignment Manual, Bureau of Public Roads, U.S. Dept. Commer., Washington, DC, USA, 1964.

[22] B. Zhou, K. Chan, T. Yu, H. Wei, J. Tang, "Strength Pareto Multigroup Search Optimizer for Multiobjective Optimal Reactive Power Dispatch," *IEEE Transactions on Industrial Informatics*, vol.10, no. 2, pp. 1012-1022, 2014.

[23] Yen, Jin Y., "Finding the K Shortest Loopless Paths in a Network." *Management Science*, vol. 17, no. 11, pp. 712-716, Jul. 1971.

[24] Simchilevi, David, and Oded Berman. "A Heuristic Algorithm for the Traveling Salesman Location Problem on Networks," *Operations Research*, vol.36, no. 3, pp. 478-484, 1988.

[25] Code for design of urban road engineering, [Online]. Available: https://wenku.baidu.com/view/10bfec74a7c30c22590102020740be1e640ecc46.html